Eigenvalue analysis of the three-dimensional tight-binding model with non-Hermitian disorder

Takamichi Terao
Department of Electrical, Electronic and Computer Engineering, Gifu University, Yanagido 1-1, Gifu 501-1193, Japan

(Received 2 March 2021; revised 24 April 2021; accepted 18 May 2021; published 1 June 2021)

In this study, the level statistics of the three-dimensional tight-binding model with non-Hermitian disorder, introduced by Tzortzakakis, Makris, and Economou (TME), and its variants were analyzed. The shift-and-invert Arnoldi method was used to analyze the eigenvalues of the TME model up to a $48 \times 48 \times 48$ cubic lattice, which was larger than those used in previous studies. The results showed that the magnitude of critical disorders in the isotropic TME model was larger than that reported in previous numerical studies for smaller systems. The localization-delocalization transition in an anisotropic model was also investigated. The computational method adopted in this study was shown to be quite effective for large-scale analysis of the calculation of all eigenvalues of sparse non-Hermitian matrices.

DOI: 10.1103/PhysRevB.103.224201

I. INTRODUCTION

In computational physics, various physical systems described by non-Hermitian matrices have attracted considerable attention [1–4]. In particular, the study of localization-delocalization transition in random non-Hermitian Hamiltonians has been of interest. In [4], the localization transitions were studied when quantum mechanical particles described by a random Schrödinger equation were subjected to a constant imaginary vector potential. In [5], the localization and delocalization in a wide class of non-Hermitian Hamiltonians were examined.

The level-spacing distribution $P(s)$ between eigenvalues has been widely used to explain the localization-delocalization transitions of wave functions in disordered systems [6–8]. The detailed properties of the level-spacing distributions have been quantitatively explained, and their relationship with random matrix theory has also been discussed [9,10]. Such spectra were characterized by a comparison with the Gaussian orthogonal ensemble in the metallic regime and the Poisson distribution in the insulating regime. These phenomena are caused by the level repulsion between adjacent eigenstates. The existence of critical-level statistics s at the mobility edge has also been explained.

Recently, the problem of level statistics on non-Hermitian disordered systems has been discussed [11,12]. Tzortzakakis, Makris, and Economou (TME) proposed a tight-binding model with real symmetric overlap energies and complex random on-site energies whose real and imaginary parts are independent random variables with uniform distribution; this is called the TME model [11]. Such a model may describe a random laser medium with balanced average random local loss and amplification. They reported the behavior of level statistics in two-dimensional systems with 50×50 square lattices. Huang and Shklovskii studied the localization-delocalization transition of a three-dimensional (3D) TME model using an exact diagonalization technique that used LAPACK [12]. The maximum system size L of their studies was 20 on a simple cubic lattice.

In general, it is desirable to perform computer simulations for large systems to investigate the localization problem of waves in disordered systems with high accuracy. Inspired by previous studies [11–13], numerical calculations from the TME model on 3D systems ($d = 3$) with a large system size were performed. The rest of the paper is organized in the following manner. In Sec. II, the model used in this study is described. In Sec. III, the numerical results are presented, and the computational method adopted in this study was shown to be quite effective for problems described in large sparse non-Hermitian matrices. In Sec. IV, the conclusions are discussed.

II. METHODS

In this study, an extended model of the original TME model [11,12] was considered. The Hamiltonian is given by

$$H = \sum_m \varepsilon_m a_m^\dagger a_m + \sum_{\langle m,n \rangle} (V_{mn} a_m^\dagger a_n + \text{H.c.}), \qquad (1)$$

where m denotes the sites on a simple cubic lattice with system size L, and the summation $\langle m, n \rangle$ is taken over the nearest-neighbor sites. The off-diagonal matrix element V_{mn} was chosen to be $V_{mn} = -V$ when sites m and n lie in the same plane perpendicular to the z axis, and $V_{mn} = -\alpha V$ ($0 < \alpha \leqslant 1$) when sites m and n lie in the z direction [14–16]. This system consists of weakly coupled planes in the z direction, and the isotropic TME model is recovered for $\alpha = 1$. Accordingly, $V = 1$ without loss of generality was chosen, and the periodic boundary conditions were applied in all directions. In Eq. (1), ε_m is the complex random on-site energy, whose real and imaginary parts are independent random variables uniformly distributed between $-W/2$ and $W/2$, where W denotes the magnitude of disorder. In an isotropic 3D system ($\alpha = 1$), the critical disorder $W = W_c$ exists, at which all eigenstates are localized in this model [12].

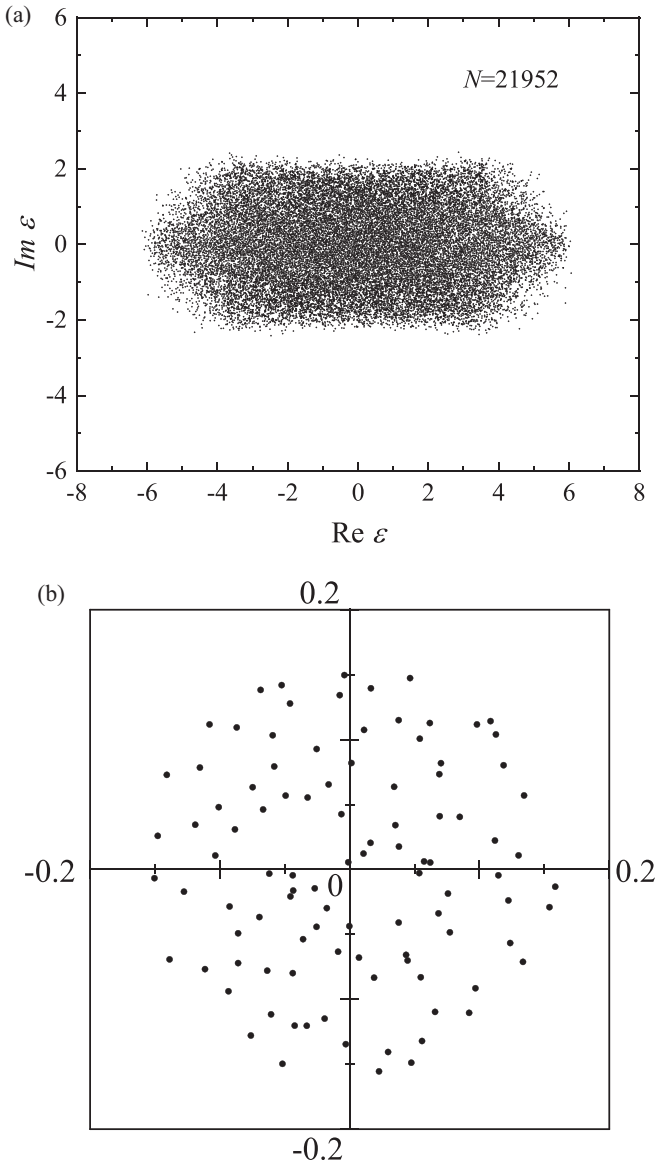

FIG. 1. (a) Example of all complex eigenvalues in the complex plane with $L = 28$ and $W = 6.0$. (b) Set of complex eigenvalues with $L = 36$ and $W = 6.0$, which shows the 100 lowest absolute values of the complex eigenvalues closest to the center of the complex plane.

III. NUMERICAL RESULTS

To perform detailed analyses on the localization-delocalization transition in disordered systems, it is necessary to introduce a computational method to efficiently analyze the eigenvalues of large-scale sparse non-Hermitian matrices. In this study, the eigenvalues of the Hamiltonian matrix [Eq. (1)] were calculated through the shift-and-invert Arnoldi method [17–19], which is suitable for obtaining the inner eigenvalues of sparse non-Hermitian matrices, to study the energy spectrum near the band center of the TME model in three dimensions. It is noteworthy that the Arnoldi method has been compared with other numerical methods in the context of Anderson localization in Hermitian systems [20].

The Arnoldi process, which is an extension of the Lanczos process, is based on Krylov subspace methods in the eigenvalue problem for unsymmetric matrices. The subspace is

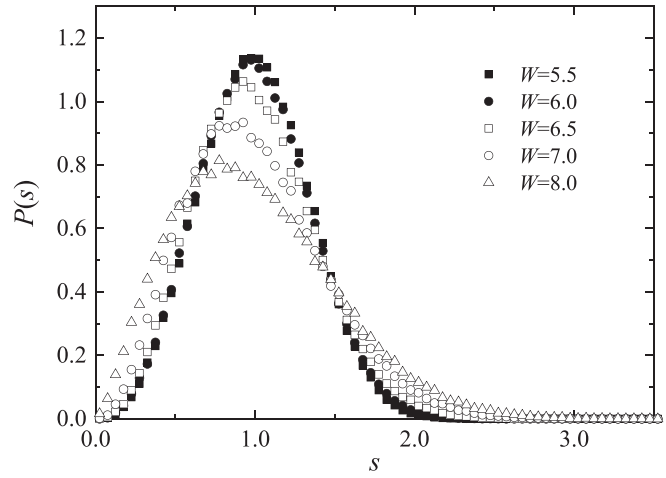

FIG. 2. $P(s)$ near the band center for different values of disorder W for $L = 20$ and $\alpha = 1.0$.

spanned by a series of vectors $\{\boldsymbol{x}_0, A\boldsymbol{x}_0, A^2\boldsymbol{x}_0, \ldots\}$, where A is a matrix of the eigenvalue problem and $\boldsymbol{x}_0$ is an arbitrary vector. The standard eigenvalue problem is written as

$$A\boldsymbol{x} = \lambda\boldsymbol{x}, \tag{2}$$

where λ and $\boldsymbol{x}$ are the eigenvalue and eigenvector, respectively. The basic Arnoldi process is described here. For an $n \times n$ matrix A, the Arnoldi vectors $\{\boldsymbol{q}_j\}$, which define an orthonormal basis for the Krylov subspace, and matrix elements $\{h_{ij}\}$ are calculated using the relationship called an m-step Arnoldi decomposition as shown below [21]:

$$A(\boldsymbol{q}_1, \boldsymbol{q}_2, \ldots, \boldsymbol{q}_m) = (\boldsymbol{q}_1, \boldsymbol{q}_2, \ldots, \boldsymbol{q}_m, \boldsymbol{q}_{m+1}) \begin{pmatrix} h_{11} & h_{12} & \cdots & \cdots & h_{1m} \\ h_{21} & h_{22} & \cdots & \cdots & h_{2m} \\ 0 & h_{32} & h_{33} & \cdots & h_{3m} \\ \vdots & & \ddots & & \vdots \\ \vdots & & & h_{mm-1} & h_{mm} \\ 0 & \cdots & \cdots & \cdots & h_{m+1\,m} \end{pmatrix}, \tag{3}$$

where $(\boldsymbol{q}_1, \boldsymbol{q}_2, \cdots, \boldsymbol{q}_m)$ is an $n \times m$ matrix composed of column vectors $\boldsymbol{q}_1, \boldsymbol{q}_2, \cdots, \boldsymbol{q}_m$. Using the relationship in Eq. (3), an $m \times m$ upper Hessenberg matrix $\tilde{H}_m$ $[(\tilde{H}_m)_{ij} = h_{ij}$ for $1 \leqslant i, j \leqslant m]$ is defined. An eigenvalue problem $\tilde{H}_m\boldsymbol{y} = \tilde{\lambda}\boldsymbol{y}$ gives an approximate solution $\tilde{\lambda}$ for the original eigenvalue λ in Eq. (2) [21,22].

In numerical calculations, the dimension m of the upper Hessenberg matrix must be sufficiently small compared to the dimension n of the original eigenvalue problem in order to reduce the memory requirement. Therefore, the implementations of the Arnoldi method requires a restarting technique, called the implicitly restarted Arnoldi method [21,23]. In addition, to obtain interior eigenvalues close to the target value σ, the shift-and-invert technique is employed as such,

$$\frac{1}{A - \sigma I}\boldsymbol{x} = \lambda'\boldsymbol{x}, \tag{4}$$

where I is a unit matrix and $\lambda' = (\lambda - \sigma)^{-1}$.

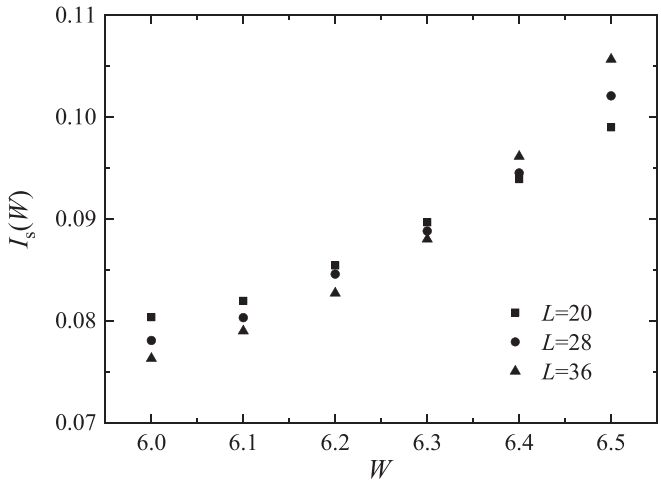

FIG. 3. W dependence of the integrated level-spacing distribution $I_S(W, L)$ plotted for three different system sizes $L =$ 20, 28, and 36.

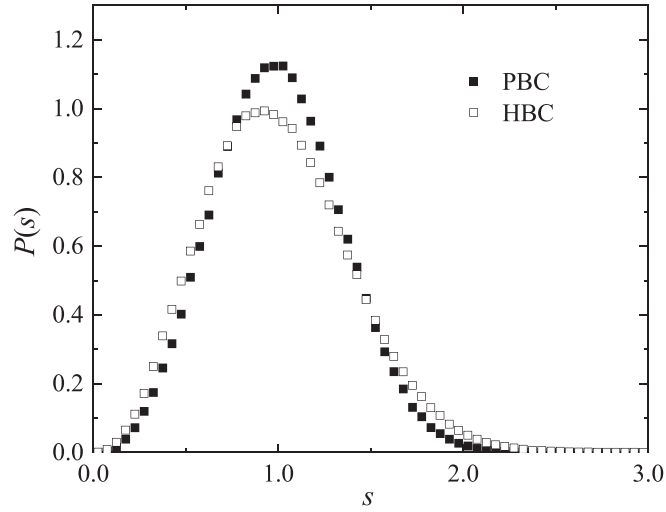

FIG. 5. Comparison of $P(s)$ for different boundary conditions, with $L = 28$ and $W = 6.0$.

First, the results for isotropic ($\alpha = 1$) systems are discussed. To understand the nature of the localization-delocalization transition and the phase diagram of the system, it is necessary to investigate not only the eigenstates near the band center but also all the eigenvalues in the complex energy plane. Therefore, a full eigenvalue analysis of the Hamiltonian matrix [Eq. (1)] was performed. Figure 1(a) shows an example of all the complex eigenvalues in the complex plane with $L = 28$ and $W = 6.0$. The abscissa and the ordinate represent the real and imaginary parts of each eigenvalue, respectively. When performing a full eigenvalue analysis of a non-Hermitian matrix, for example by applying the QR method [21], it takes a computation time of order N^3, where N is the order of the matrix, and such numerical methods for non-Hermitian matrices are generally not suitable for parallel computations. Therefore, the CPU time increases rapidly as the order of the matrix N increases. In the shift-and-invert Arnoldi method, independent parallel computations with the shifted values in the complex eigenvalue plane become possible, and all eigenvalue analyses of large-scale non-Hermitian matrices can be easily performed. In the eigenvalue analysis, a target value in the complex plane was specified, and a limited number of complex eigenvalues in the vicinity of each target value were numerically obtained. To calculate all eigenvalues of the system, many different target values were considered in the entire region of the complex plane where the eigenvalues were believed to appear. By performing eigenvalue calculations on all of them and collecting the results obtained, it was confirmed that all eigenvalues of the matrix were obtained. Figure 1(b) shows an example of a group of complex eigenvalues with $L = 36$ and $W = 6.0$, where the 100 lowest absolute values of the complex eigenvalues closest to the center of the complex plane are plotted. Figure 2 shows $P(s)$ near the band center for different values of disorder W for $L = 20$. In this model, the value of s corresponds to the distance from a given eigenvalue to its first nearest eigenvalue on the complex plane. When W increases, the profile of $P(s)$ broadens, and these overall features are in agreement with those of a previous study [12], where $P(s)$ for different W values intersect near

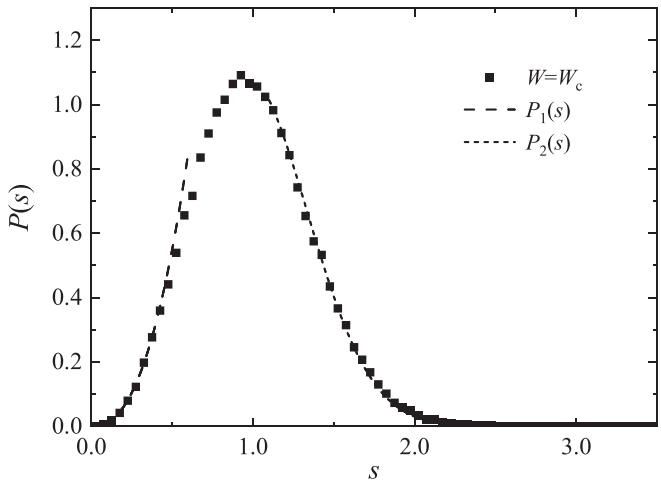

FIG. 4. Profile of the critical level statistics $P(s)$ with $L = 48$ and $W = 6.35$.

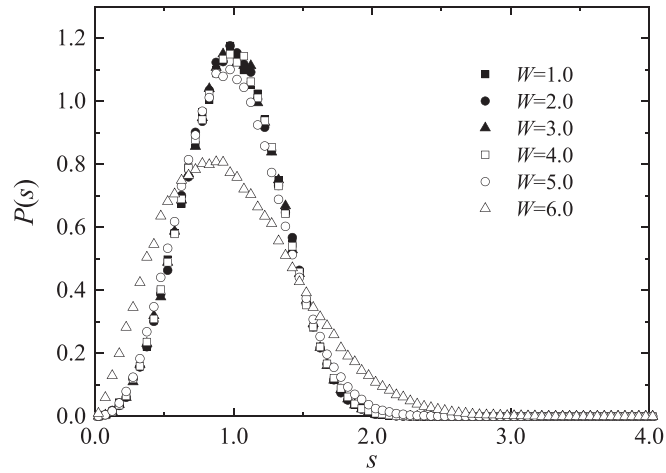

FIG. 6. $P(s)$ near the band center for different values of disorder W for $L = 28$ and $\alpha = 0.5$.

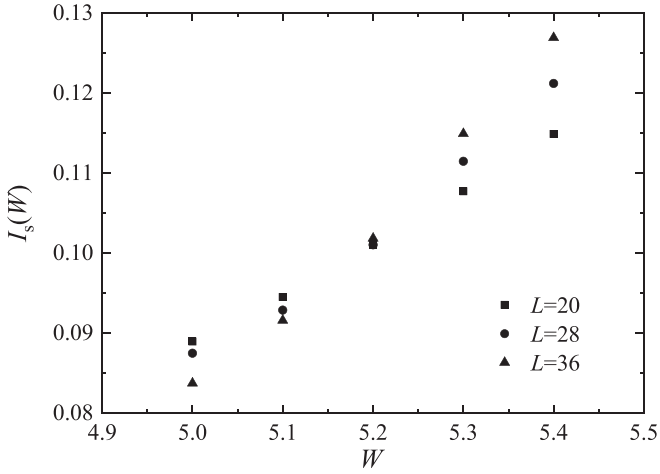

FIG. 7. W dependence of the integrated level-spacing distribution $I_S(W, L)$ with $\alpha = 0.5$.

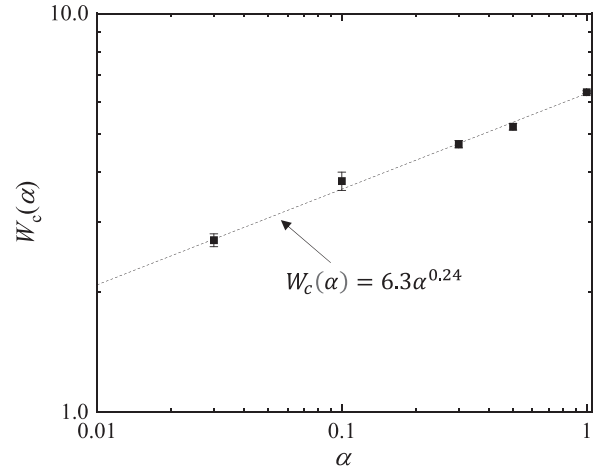

FIG. 8. α dependence of the critical disorder $W_c(\alpha)$.

$s \approx 1.5$. This is apparently different from the 3D Anderson model ($s \approx 2.0$) [6,7].

Hofstetter and Schreiber [8] and Zharekeshev and Kramer [6] studied the integrated level-spacing distribution to detect the critical behavior during the disorder-induced metal-insulator transition in a 3D Anderson model. The integrated level-spacing distribution $I_S(W, L)$ is defined as

$$I_S(W, L) = \int_{\gamma}^{\infty} P(s)\, ds. \tag{5}$$

To select the lower limit of integration γ in Eq. (5), it is sufficient to choose a value that makes it possible to distinguish between localized and delocalized states. In the following, the lower limit of the integral γ is assumed to be $\gamma = 1.5$. In Fig. 3, the W dependence of $I_S(W, L)$ is plotted with respect to three different values of L, i.e., 20, 28, and 36. $P(s)$ is expected to show no size dependence during the localization-delocalization transition, which is called critical-level statistics. As a result, $I_S(W, L)$ is considered independent of L for $W = W_c$. From the present calculations, it is concluded that the value of W_c falls in the range $6.3 < W_c < 6.4$. The abovementioned value is slightly larger than $W_c \approx 6.0$, as reported in a previous study [12]. In Fig. 4, the profile of the critical level statistics $P(s)$ with $L = 48$ and $W = 6.35$ is shown in a log-log plot. Although it is difficult to fit the entire region within a single curve, the numerical results mostly obey the asymptotic form, e.g., the profile being a power-law function $P_1(s) \approx 2.9s^{2.4}$ for $s \ll 1$ (long dashed line in Fig. 4) and a Gaussian function $P_2(s) \approx 1.1e^{-3.2(s-0.94)^2}$ for $s \gg 1$ (short dashed line in Fig. 4).

The values of W_c in this study and that in [12] are not in agreement with each other. The effect of different boundary conditions on the probability density $P(s)$ was also tested on the TME model in three dimensions. With $L = 28$ and $W = 6.0$, the results of the comparison of $P(s)$ with periodic boundary conditions (PBCs) and that with hard-wall boundary conditions (HBCs) are shown in Fig. 5. The results indicate that the boundary condition clearly affects $P(s)$. With HBCs, some of the eigenvectors may become spatially localized modes at the edge of the system. This will affect the statistical properties of the eigenvalue spectrum in the system, and the value of W_c will change for different boundary conditions.

Similarly, for the Hamiltonian in Eq. (1), the results for an anisotropic system ($\alpha \neq 1$) were also shown. The $\alpha \to 0$ limit corresponds to the TME model in 2D systems, where no evidence of localization-delocalization transition has been found [12]. Figure 6 shows $P(s)$ near the band center for different values of disorder W for $L = 28$ and $\alpha = 0.5$. It was shown again that the $P(s)$ for different W values intersect. The calculation result of $I_S(W, L)$ for the anisotropic system ($\alpha = 0.5$) is shown in Fig. 7. For the lower integral limit γ in Eq. (2), the same value as in the analysis of the isotropic system ($\alpha = 1.0$) was used. $I_S(W, L)$ was considered to be independent of L for $W = W_c$, and $W_c = 5.2 \pm 0.1$. The value of W_c in the anisotropic system was smaller than $W_c = 6.35 \pm 0.05$ in the isotropic system. It is interesting to examine other values of α as an attempt to find how the critical disorder $W_c = W_c(\alpha)$ depends on the parameter α in the range $0<\alpha<1$. Figure 8 shows the calculated results of α dependence on the critical disorder $W_c(\alpha)$. It is evident that the value of $W_c(\alpha)$ decreases with α according to the power law $W_c(\alpha) = 6.3\alpha^{0.24}$, which is shown by a dashed line. This is reminiscent of the result $W_c(\alpha) = 16.5\alpha^{0.25}$ in the three-dimensional Anderson model with anisotropy [16] - the power-law exponents in both cases are nearly identical.

IV. CONCLUSIONS

In this study, the level statistics s of the 3D TME model and its variants in anisotropic systems were analyzed. By using the shift-and-invert Arnoldi method, all eigenvalue analyses were performed, and the eigenvalue distribution of this model was explained on the complex energy plane. An eigenvalue analysis for TME models larger than those used in previous studies was performed, and the mobility edges of these systems were investigated quantitatively. The results show that $W_c = 6.35 \pm 0.05$ for the isotropic TME model. With increasing anisotropy, the critical disorder $W_c(\alpha)$ decreases according to the power law $W_c(\alpha) = 6.3\alpha^{0.24}$.

In general, in the large-scale eigenvalue analysis of non-Hermitian matrices, ill-conditioned problems are often

encountered, unlike those of Hermitian matrices, and iterative methods developed for large-scale Hermitian sparse matrices are not always effective. Therefore, it is expected that large-scale numerical studies based on the approach proposed in this study will provide useful insights into various problems described by non-Hermitian matrices, which have recently attracted much interest.

ACKNOWLEDGMENTS

I would like to thank the Supercomputer Center at the Institute for Solid State Physics, University of Tokyo, for their facilities. This work was supported by JSPS KAKENHI (Grants-in-Aid for Scientific Research by JSPS) Grant No. 20K11848.

[1] K. Rajan and L. F. Abbott, Phys. Rev. Lett. **97**, 188104 (2006).
[2] G. H. Zhang and D. R. Nelson, Phys. Rev. E **100**, 052315 (2019).
[3] T. Terao, Phys. Rev. E **82**, 026702 (2010).
[4] N. Hatano and D. R. Nelson, Phys. Rev. Lett. **77**, 570 (1996).
[5] J. Feinberg and A. Zee, Phys. Rev. E **59**, 6433 (1999).
[6] I. Kh. Zharekeshev and B. Kramer, Phys. Rev. B **51**, 17239 (1995).
[7] E. Hofstetter and M. Schreiber, Phys. Rev. B **48**, 16979 (1993).
[8] E. Hofstetter and M. Schreiber, Phys. Rev. B **49**, 14726 (1994).
[9] M. L. Mehta, *Random Matrices*, 2nd ed. (Academic Press, San Diego, 1991).
[10] F. L. Metz, I. Neri, and T. Rogers, J. Phys. A: Math. Theor. **52**, 434003 (2019).
[11] A. F. Tzortzakakis, K. G. Makris, and E. N. Economou, Phys. Rev. B **101**, 014202 (2020).
[12] Y. Huang and B. I. Shklovskii, Phys. Rev. B **101**, 014204 (2020).
[13] Y. Huang and B. I. Shklovskii, Phys. Rev. B **102**, 064212 (2020).
[14] F. Milde, R. A. Römer, and M. Schreiber, Phys. Rev. B **55**, 9463 (1997).
[15] Qiming Li, C. M. Soukoulis, E. N. Economou, and G. S. Grest, Phys. Rev. B **40**, 2825 (1989).
[16] F. Milde, R. A. Römer, and M. Schreiber, Phys. Rev. B **61**, 6028 (2000).
[17] F. Chatelin, *Eigenvalues of Matrices* (SIAM, Philadelphia, 2012).
[18] R. B. Lehoucq, D. C. Sorensen, and C. Yang, *Users' Guide: Solution of Large-scale Eigenvalue Problems with Implicitly Restarted Arnoldi Methods* (SIAM, Philadelphia, 1998).
[19] P. Virtanen, R. Gommers, T. E. Oliphant, M. Haberland, T. Reddy, D. Cournapeau *et al.*, Nat. Methods. **17**, 261 (2020).
[20] U. Elsner, V. Mehrmann, F. Milde, R. A. Römer, and M. Schreiber, SIAM J. Sci. Comput. **20**, 2089 (1999).
[21] G. H. Golub and C. F. van Loan, *Matrix Computations,* 4th ed. (John Hopkins, Baltimore, Maryland, 2013).
[22] Y. Saad, *Iterative Methods for Sparse Linear Systems,* 2nd ed. (SIAM, Philadelphia, 2003).
[23] D. C. Sorensen, SIAM J. Matrix Anal. Appl. **13**, 357 (1992).